THE JOURNAL OF BIOLOGICAL CHEMISTRY
Vol. 274, No. 14, Issue of April 2, pp. 9854–9860, 1999

Printed in U.S.A.

Selective Perturbation of Early Endosome and/or *trans*-Golgi Network pH but Not Lysosome pH by Dose-dependent Expression of Influenza M2 Protein*

(Received for publication, December 22, 1998, and in revised form, January 26, 1999)

Jennifer R. Henkel‡, Jamie L. Popovich‡, Gregory A. Gibson‡, Simon C. Watkins§, and Ora A. Weisz‡¶

From the ‡Laboratory of Epithelial Cell Biology, Renal-Electrolyte Division and §Department of Cell Biology and Physiology, University of Pittsburgh, Pittsburgh, Pennsylvania 15213

Many sorting stations along the biosynthetic and endocytic pathways are acidified, suggesting a role for pH regulation in protein traffic. However, the function of acidification in individual compartments has been difficult to examine because global pH perturbants affect all acidified organelles in the cell and also have numerous side effects. To circumvent this problem, we have developed a method to selectively perturb the pH of a subset of acidified compartments. We infected HeLa cells with a recombinant adenovirus encoding influenza virus M2 protein (an acid-activated ion channel that dissipates proton gradients across membranes) and measured the effects on various steps in protein transport. At low multiplicity of infection (m.o.i.), delivery of influenza hemagglutinin from the *trans*-Golgi network to the cell surface was blocked, but there was almost no effect on the rate of recycling of internalized transferrin. At higher m.o.i., transferrin recycling was inhibited, suggesting increased accumulation of M2 in endosomes. Interestingly, even at the higher m.o.i., M2 expression had no effect on lysosome morphology or on EGF degradation, suggesting that lysosomal pH was not compromised by M2 expression. However, delivery of newly synthesized cathepsin D to lysosomes was slowed in cells expressing active M2, suggesting that acidification of the TGN and endosomes is important for efficient delivery of lysosomal hydrolases. Fluorescence labeling using a pH-sensitive dye confirmed the reversible effect of M2 on the pH of a subset of acidified compartments in the cell. The ability to dissect the role of acidification in individual steps of a complex pathway should be useful for numerous other studies on protein processing and transport.

Protein sorting along the biosynthetic and endocytic pathways of cells is a complex event whose specificities are just beginning to be understood. Intriguingly, some of the major sorting stations in cells, the *trans*-Golgi network (TGN)[1] and endosomes, are known to be acidified, and pH regulation is known to be required for some functions of these organelles. For example, acidic pH is required for the proper sorting and processing of regulated secretory proteins and hormones in the TGN of endocrine cells (1, 2). Furthermore, acidification of early endosomes is thought to be necessary for the dissociation of some internalized ligands from their receptors (3). However, outside of a few specific examples, the role of acidification in protein trafficking is not well understood. In part, this is due to the inherent problems presented by the use of global pH perturbants such as weak bases or the vacuolar H^+-ATPase (V-ATPase) inhibitors bafilomycin A_1 ($BafA_1$) and concanamycins A and B. These inhibitors disrupt the pH of all acidified compartments in the cell, have dramatic effects on organelle morphology, and are only slowly reversible. In addition, $BafA_1$ may differentially affect V-ATPase isoforms in some organelles, further complicating interpretation of results (4, 5). Moreover, at least some cells can become rapidly resistant to treatment with concanamycin (6). Together these complications may account for the vast discrepancies between different studies on the effects on biosynthetic and endocytic traffic when acidification is disrupted (7–15).

We have taken a different approach to dissect the function of acidification in transport through individual compartments in the cell. We have expressed the M2 protein of influenza virus in cells and examined its effects on transport. M2 is an acid-activated proton-selective channel formed by the self-association of 97 amino acid single membrane-spanning proteins into tetramers (16–20). M2 activity is controlled by the pH-dependent protonation state of a transmembrane histidine residue (21). Unlike global perturbants, M2 expression should affect the pH of only those acidified compartments in which it is present. Moreover, M2 activity and its effects on transport can be rapidly and reversibly modulated using the specific ion channel blocker BL-1743 (22–24).

Previously, we demonstrated that intracellular M2 is localized to the TGN and apical recycling endosomes of polarized Madin-Darby canine kidney cells and selectively affects transport of itinerant proteins through these but not through other normally acidified compartments (24).[2] Here we have expanded our studies to examine the effects of M2 on nonpolarized cells. Interestingly, in these cells we find that the effect of M2 in different subcellular compartments can be controlled by adjusting the expression level of M2. Furthermore, we can rapidly

* This work was supported by National Institutes of Health Grant R01DK54407 and by grants from the Cystic Fibrosis Foundation, the Competitive Medical Research Fund of the University of Pittsburgh, and the Emma and Samuel Winters Foundation (to O. A. W.). The Laboratory of Epithelial Cell Biology is supported in part by Dialysis Clinic Inc. The costs of publication of this article were defrayed in part by the payment of page charges. This article must therefore be hereby marked "*advertisement*" in accordance with 18 U.S.C. Section 1734 solely to indicate this fact.

¶ To whom correspondence should be addressed: Renal-Electrolyte Division, University of Pittsburgh, 978 Scaife Hall, 3550 Terrace St., Pittsburgh, PA 15213. Tel.: 412-383-8891; Fax: 412-383-8956; E-mail: weisz@med1.dept-med.pitt.edu.

[1] The abbreviations used are: TGN, *trans*-Golgi network; AMT, amantadine; AV, adenovirus; $BafA_1$, bafilomycin A_1; EGF, epidermal growth factor; HA, influenza hemagglutinin; MPR, mannose 6-phosphate receptor; PBS, phosphate-buffered saline; Tf, transferrin; V-ATPase, vacuolar H^+-ATPase; m.o.i., multiplicity of infection; BSA, bovine serum albumin; MEM, minimal essential medium.

[2] J. R. Henkel and O. A. Weisz, unpublished observations.

and reversibly inactivate M2 ion channel activity. This flexibility makes M2 expression a useful tool with which to probe the role of acidification in protein sorting and delivery.

EXPERIMENTAL PROCEDURES

Cell Culture and Adenoviral Infection—HeLa cells were maintained in Dulbecco's modified Eagle's medium supplemented with 10% fetal bovine serum. Generation and characterization of E1-substituted recombinant adenoviruses encoding Rostock M2 in the correct and reverse orientations (AV-M2 and AV-M2rev, respectively), influenza hemagglutinin (AV-HA), and the tetracycline transactivator (AV-TA) are described in Ref. 24. Cells were plated (3×10^5/35-mm dish or 1×10^5/12-mm well) the day before infection. Cells were washed with calcium-free phosphate-buffered saline containing 1 mM $MgCl_2$ (PBS-M). After 5 min at room temperature, the PBS-M was removed, and 400 μl of PBS-M (200 μl for 12-mm wells) containing recombinant adenovirus was added. Cells infected with AV-M2 at a multiplicity of infection (m.o.i.) of 100 received AV-TA at a m.o.i. of 50, whereas cells infected with AV-M2 at a m.o.i. of 500 received AV-TA at a m.o.i. of 100. The dishes were rocked briefly by hand, and the cells were returned to the incubator for 1–2 h. Mock-infected cells were treated identically except that virus was omitted during the incubation period. Dishes were then rinsed with PBS-M, and cells were incubated overnight in growth medium. The M2 ion channel inhibitors amantadine (AMT, Sigma; 5 μM) or BL-1743 (gift of Dr. Mark Krystal, Bristol-Myers Squibb Pharmaceutical Research Institute, Wallingford, CT; 5 μM) were added as 1000-fold concentrated stocks prepared in 95% ethanol at this step or in subsequent steps where indicated to inhibit M2 activity. Experiments were initiated at 18–24 h postinfection.

Cell Surface Delivery of HA—Surface delivery of newly synthesized HA was performed as described in (23) with minor modifications. Cells were coinfected with AV-M2 or AV-M2rev, AV-TA, and AV-HA (m.o.i. 40) as described above. The following day, cells were rinsed once with PBS, then starved for 30 min in medium A (cysteine-free, methionine-free MEM containing 0.35 g/liter $NaHCO_3$, 10 mM HEPES, and 10 mM MES, pH 7.0; Ref. 25). AMT was added to the indicated samples at the beginning of the starvation and included during the pulse and chase periods. Cells were metabolically labeled with 50–100 μCi/ml EXPRE^{35}S^{35}S (NEN Life Science Products) in the same medium, then chased for 2 h at 19 °C in the same medium supplemented with four times the normal amount of cysteine and methionine (medium B). At various times, dishes were removed, rapidly chilled to 0 °C by rinsing with ice-cold PBS, and incubated on ice for 30 min in 1 ml medium B containing 100 μg/ml L-1-tosylamido-2-phenylethyl chloromethyl ketone-treated trypsin (Sigma) for 30 min. Trypsin cleaves HA into two subunits (HA1 and HA2) that remain associated via disulfide bonds during immunoprecipitation. Trypsinization was stopped by incubating the cells twice for 10 min with ice-cold medium B containing 200 μg/ml soybean trypsin inhibitor (Sigma). Cells were then rinsed with PBS and lysed in 0.5 ml of detergent solution (50 mM Tris-HCl, 2% Nonidet P-40, 0.4% deoxycholate, 62.5 mM EDTA, pH 8.0) containing 0.13 TIU/ml aprotinin and 20 μg/ml soybean trypsin inhibitor. Lysates were centrifuged briefly to remove nuclei, and SDS was added to the supernatant to a final concentration of 0.2%. HA was immunoprecipitated using monoclonal antibody Fc125 (23), and antibody-antigen complexes were collected using fixed *Staphylococcus aureus* (Calbiochem). Where indicated, samples were treated with endoglycosidase H (New England Biolabs, Beverly, MA) as described previously (23). After electrophoresis on 10% SDS-polyacrylamide gels, the percentage of cleaved HA was quantitated using a phosphorimager (GS-363 Molecular Imager System, Bio-Rad).

Transferrin Recycling Assays—HeLa cells were mock-infected or infected with recombinant adenovirus as described above. The following day, cells were depleted of intracellular stores of transferrin (Tf) by incubation for 1 h at 37 °C in MEM/BSA (MEM, Hanks' balanced salt solution, 0.6% BSA, 20 mM HEPES, pH 7.4) and ^{125}I-labeled iron-loaded human Tf (~5 μg/ml; ~5×10^6 cpm/μg) was internalized for 45 min at 37 °C. The cells were washed three times rapidly and twice for 5 min each with ice-cold MEM/BSA, then incubated at 37 °C for 2.5 min to allow receptor internalization. The medium was replaced with prewarmed MEM/BSA and the cells incubated at 37 °C. At the designated times, the medium was collected and replaced. After the final time point, cells were lysed in detergent solution and the amount of ^{125}I-labeled Tf in all samples was determined using a γ counter (Packard Instrument Co., Downers Grove, IL). The kinetics of transferrin recycling were calculated by determining the cumulative percentage of preinternalized transferrin released into the medium at each time point.

EGF Degradation—HeLa cells were mock-infected or infected with recombinant adenovirus as described above. AMT was added to the indicated samples immediately after infection and included in subsequent steps. The following day, cells were incubated with ^{125}I-labeled EGF (0.5 μM in MEM/BSA; Amersham Pharmacia Biotech) for 2 h at 0 °C. Cells were washed three times on ice for five min each with MEM/BSA, rinsed an additional three times, and then incubated with prewarmed medium. Chloroquine (50 μg/ml) was added to the indicated samples at this time. At various times, the medium was collected and replaced; at the end of the time course, the cells were solubilized with 1% Triton X-100 in 50 mM Tris, pH 7.4. trichloroacetic acid (10% final concentration added as a 100% w/v stock; Sigma) was added, and the samples were incubated on ice for 10 min. Samples were then centrifuged at maximum speed in a microcentrifuge for 15 min at 4 °C, and the radioactivity in the supernatants and pellets counted using a γ counter. The rate of EGF degradation was determined by calculating the cumulative release of trichloroacetic acid-soluble counts into the medium over time.

Indirect Immunofluorescence—Indirect immunofluorescence of HeLa cells was performed as described previously (23). Briefly, cells were rinsed once with PBS, fixed for 20 min at ambient temperature in 3% paraformaldehyde, then incubated briefly with PBS containing 10 mM glycine and 0.02% sodium azide (PBS-G). Where indicated, cells were permeabilized for 3 min in 0.5% Triton X-100 in PBS-G. Nonspecific binding was blocked with 0.25% ovalbumin in PBS-G prior to incubation with antibodies. M2 was detected using the monoclonal antibody 5C4 (a generous gift of Dr. Robert Lamb, Northwestern University) at a dilution of 1:250 followed by Cy3-conjugated affinity-purified goat anti-mouse IgG (2 mg/ml, 1:1000 dilution; Jackson ImmunoResearch Laboratories, Inc., Avondale, PA). Cells were viewed using a Nikon Optiphot microscope (Fryer Company, Inc., Carpentersville, IL) and images were acquired using a Hamamatsu C5985 chilled CCD camera (8 bit, 756 × 483 pixels; Hamamatsu Photonics Systems, Bridgewater, NJ).

Fluorescence Imaging in Live Cells—To qualitatively assess the effect of M2 expression on organelle pH, we incubated mock- or AV-M2-infected HeLa cells with 5 μM LysoSensor (Molecular Probes, Eugene, OR) in MEM/BSA. Acidified compartments were visualized using an Olympus Provis microscope (Olympus, Tokyo, Japan) using a triple pass (blue/green/red) cube, which allows excitation at 384 nm and collection at 540 nm. Images were collected digitally to a Sony 3 chip color CCD camera (Sony 970; Sony Electronics, Tokyo, Japan) equipped with hardwired on chip integration circuitry. In each experiment images were collected over 256 grayscales for each color, for 3 video frames. The effects of chloroquine (200 μg/ml) and AMT (10 μM) on the fluorescence patterns of mock-infected and M2-expressing samples were determined after 1-h and 15-min incubations, respectively.

Cathepsin D Processing—HeLa cells cultured in 35-mm dishes were infected with adenoviruses as described above. The following day, cells were starved, radiolabeled for 20 min with 100 μCi/ml [^{35}S]methionine in medium A, then chased for the indicated times in medium B. The medium was collected and a 5-fold concentrated stock of detergent solution supplemented with aprotinin was added to a final concentration of 1×. Cells were solubilized in detergent solution as described above and samples were incubated with anti-cathepsin D antibody (Calbiochem). Antibody-antigen complexes were collected using fixed *S. aureus* and analyzed on 12% SDS-polyacrylamide gel electrophoresis gels.

RESULTS

M2 Slows TGN-to-Cell Surface Delivery of Influenza Hemagglutinin—Our previous results demonstrated that vaccinia virus mediated overexpression of M2 inhibited TGN to surface delivery of influenza HA (23). However, at these extremely high expression levels, M2 also inhibited earlier steps in transport through nonacidified compartments (23, 25). Moreover, in our hands, synchronization of proteins along the secretory pathway by temperature blocks is not effective in vaccinia infected cells. To circumvent these problems we developed replication-defective recombinant adenoviruses expressing M2 (AV-M2) (24). In our system, expression of M2 is driven by the tetracycline operon and thus requires coinfection with an adenovirus encoding the tetracycline transactivator chimera (AV-TA; expression of the TA protein in this virus is constitutively driven by

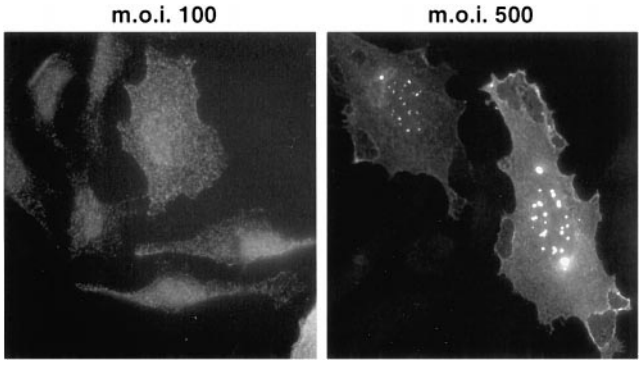

FIG. 1. **Distribution of adenovirally expressed M2 in HeLa cells.** HeLa cells were infected with AV-TA and AV-M2 or AV-M2rev at the indicated m.o.i. The following day, cells were fixed, permeabilized, and processed for indirect immunofluorescence to localize M2. Very little M2 expression was detected in cells infected at low m.o.i., and more was observed at the higher expression level.

the constitutive CMV promoter). We infected HeLa cells using AV-M2 and AV-TA at various m.o.i. and examined the localization of the protein using indirect immunofluorescence (Fig. 1). Cells infected at low m.o.i. (100) had very low levels of M2 staining. More staining was visible in cells infected with AV-M2 at m.o.i. 500. Interestingly, most of the staining was localized to the plasma membrane, and no distinct organelle staining was visible at either infection level. However, the nuclei of many of the cells infected at high m.o.i. had multiple donut-shaped inclusions that stained brightly for M2. The origin of these inclusions is not known. Other than this, we did not observe any effect of viral infection on the morphology of the cells during the course of our experiments. These expression patterns are very different from M2 overexpressed in HeLa cells using recombinant vaccinia, where the majority of the protein accumulated in the endoplasmic reticulum and Golgi complex and cells became rounded after several hours of expression (23).

To test the effect of M2 on biosynthetic traffic, we infected HeLa cells at various m.o.i. with AV-TA and AV-M2 (or AV-M2rev, a control virus that encodes M2 in the reverse orientation) and measured the effects on HA delivery from the TGN to the plasma membrane. Cells were radiolabeled for 15 min, then chased for 2 h at 19 °C to accumulate newly synthesized proteins in the TGN. M2 had a moderate effect on the amount of HA that was endoglycosidase H-resistant after this chase period, consistent with slower intra-Golgi transport as has been reported previously (23, 25) (Fig. 2*A*). Similar effects on early Golgi transport have been documented using other pH perturbants (8–10). We have demonstrated previously that the delay in these early transport steps in M2-expressing cells is most likely an indirect effect resulting from prolonged accumulation of proteins, lipids, and possibly transport machinery in the TGN (23). As expected, M2 expression had a much more dramatic effect on the kinetics of HA delivery from the TGN to the plasma membrane (Fig. 2, *B* and *C*). The effect of M2 on HA delivery was maximal at m.o.i. 100. Subsequent experiments showed similar inhibition at m.o.i. as low as 50 (data not shown). These results suggest that M2 is active in the TGN, and that TGN acidification is required for efficient delivery of HA to the cell surface in these cells.

M2 Expression Causes Dose-dependent Inhibition of Transferrin Recycling—We then measured the effect of M2 expression on Tf recycling. In polarized Madin-Darby canine kidney cells, where M2 expression is restricted to apical endosomal compartments, we observed no effect on Tf recycling (24). However, we reasoned that M2 might affect Tf recycling if it localized to endosomal compartments in nonpolarized cells. Thus, we determined the effect of increasing M2 expression levels on Tf recycling (Fig. 3). Cells infected with M2rev had identical Tf

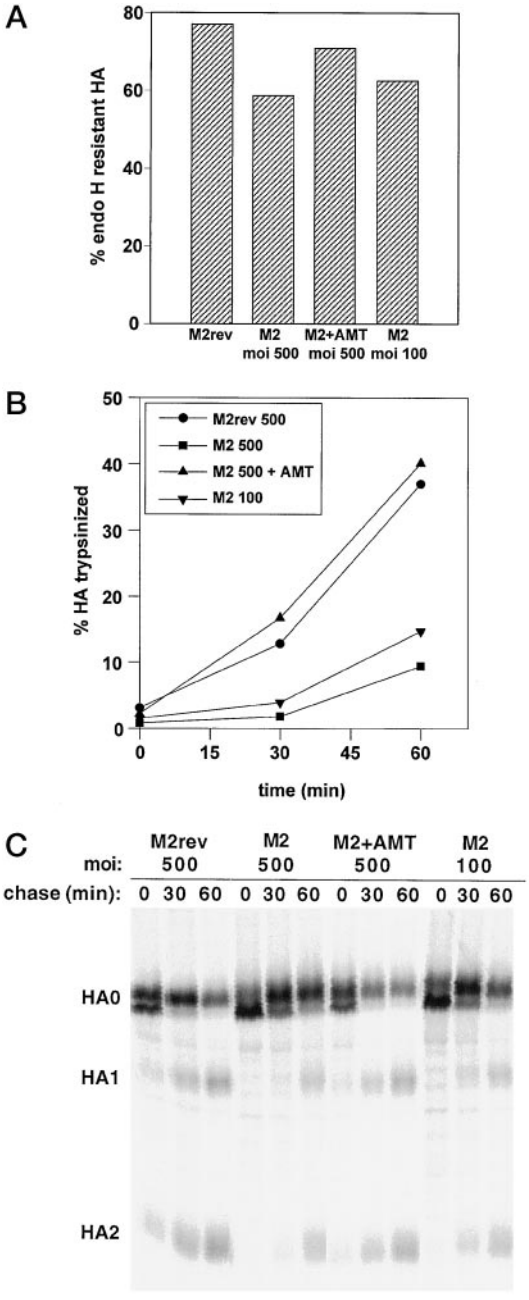

FIG. 2. **M2 blocks delivery of HA to the plasma membrane.** *A*, M2 expression slows arrival of HA to the *medial* Golgi. HeLa cells were infected with AV-M2 or AV-M2rev, AV-TA, and AV-HA as described under "Experimental Procedures." The following day, cells were metabolically radiolabeled for 15 min, then chased for 2 h at 19 °C (in the presence or absence of AMT). Samples were solubilized, immunoprecipitated with anti-HA antibody, and treated with endoglycosidase H (*endo H*) to determine the amount of HA reaching the medial Golgi during the chase period. *B* and *C*, M2 markedly slows TGN-to-cell surface delivery of HA. HeLa cells infected with AV-M2 or AV-M2rev and AV-TA were metabolically radiolabeled and chased for 2 h at 19 °C as above to accumulate newly synthesized HA in the TGN. AMT was included in the indicated dishes throughout the pulse/chase to block M2 ion channel activity. The cells were then rapidly warmed to 37 °C and the kinetics of HA delivery to the plasma membrane determined using cell surface trypsinization as described under "Experimental Procedures." The positions of intact HA (*HA0*) and its trypsin cleavage products (*HA1* and *HA2*) are marked. Quantitation of the gel in *C* is shown in *B*. Similar results were obtained in three experiments.

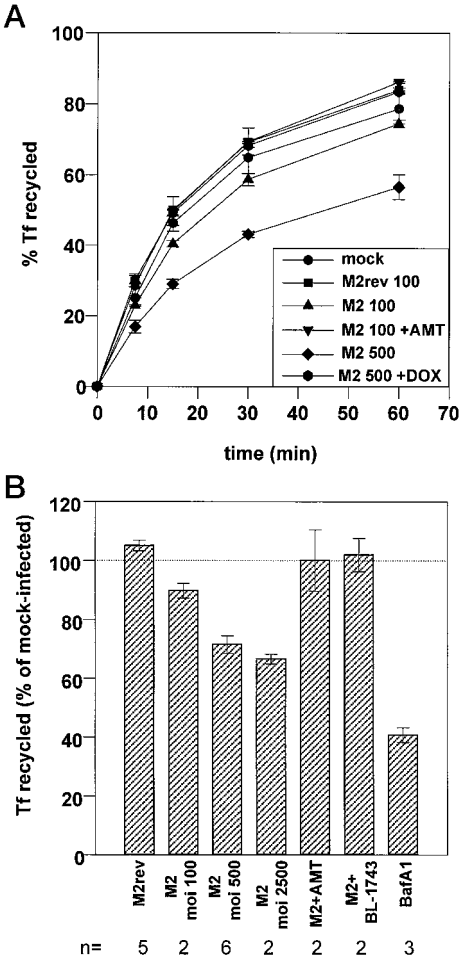

FIG. 3. **M2 expression causes dose-dependent inhibition of transferrin recycling.** *A*, effect of M2 on transferrin recycling kinetics. HeLa cells infected with AV-M2 or AV-M2rev at the indicated m.o.i. were incubated with ^{125}I-labeled Tf for 45 min, then washed extensively, and the kinetics of transferrin release into the medium quantitated. AMT or doxycycline (*DOX*) were included in the indicated samples to block M2 activity and expression, respectively. The mean ± S.D. of triplicate samples is plotted. *B*, summary of the effects of M2 on transferrin recycling. HeLa cells were infected with the AV-M2rev (m.o.i. 100–2500) or AV-M2 and transferrin recycling monitored as described under "Experimental Procedures." AMT or the reversible M2 inhibitor BL-1743 were included in the indicated samples to block M2 activity. Some mock-infected cells were pretreated with 0.5 μM $BafA_1$ for 30 min prior to transferrin uptake. The amount of transferrin released into the medium after 15-min chase is plotted as a percentage of release from mock-infected cells. The number (n) of times an experiment was performed is shown for each condition, and the mean ± S.E. ($n > 2$) or range ($n = 2$) is plotted.

recycling kinetics compared with mock-infected cells (Fig. 3*A*). M2 expressed using low m.o.i. (100) had a slight but reproducible effect on Tf recycling (~10% decrease in initial rate). By contrast, Tf recycling was markedly reduced (~30%) in cells expressing higher levels of M2 (m.o.i. 500). Addition of doxycycline to block M2 expression after viral infection, or addition of AMT to the medium shortly before Tf uptake, resulted in normal Tf recycling kinetics, suggesting that the effect on recycling was due to M2-mediated ion channel activity. Fig. 3*B* shows the results from several experiments in which the dose-dependence of M2's effect on Tf recycling was compared. The effect of M2 on Tf recycling was essentially maximal at m.o.i. 500, as increasing the dose to m.o.i. 2500 had no further effect on recycling. Interestingly, the effect of M2 on recycling never approached that of the V-ATPase inhibitor $BafA_1$, which inhibited recycling by approximately 60%. Addition of AMT or the reversible M2 inhibitor BL-1743 completely blocked the effect of M2 at all m.o.i. tested.

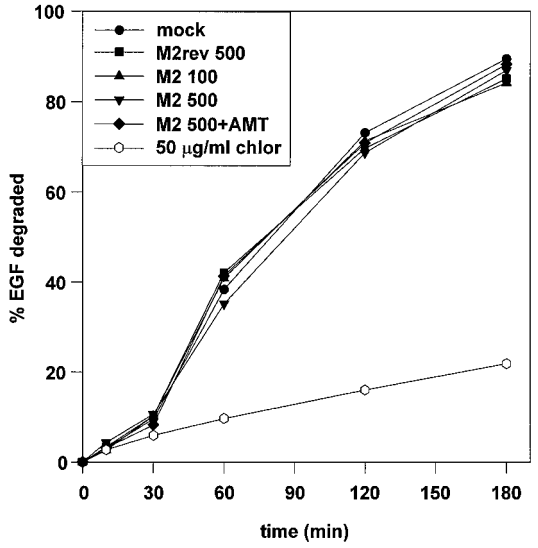

FIG. 4. **M2 expression does not affect EGF degradation.** HeLa cells (mock-infected or infected with AV-TA and AV-M2rev or AV-M2 at the indicated m.o.i.) were incubated with ^{125}I-labeled EGF on ice for 2 h. The cells were then washed extensively, then rapidly warmed, and the kinetics of EGF degradation measured as described under "Experimental Procedures." Indicated samples were treated with AMT (5 μM) or 50 μg/ml chloroquine (*chlor*). Similar results were obtained in three independent experiments.

M2 Expression Does Not Affect Lysosomal pH—To test whether M2 expression affected lysosomal function, we measured its effect on degradation of radioiodinated EGF. Interestingly, no effect of M2 on EGF degradation was observed, whereas treatment with chloroquine drastically inhibited this process (Fig. 4). To further confirm that M2 did not disrupt lysosomal pH, we compared the effects of M2 and chloroquine on lysosome morphology using indirect immunofluorescence (Fig. 5). As expected, incubation with chloroquine caused dramatic swelling of lysosomal compartments as visualized using an antibody against the membrane protein LAMP-1. By contrast, M2 expression had no effect on LAMP-1 staining.

Although there is considerable indirect evidence to suggest that M2 expression alters organelle pH, this has never been directly measured (26–30). We took advantage of a relatively new fluorescence pH indicator to test whether M2 affected the pH of intracellular organelles. We incubated mock-infected or AV-M2-infected HeLa cells (m.o.i. 500) with LysoSensor yellow/blue, a membrane permeant probe that fluoresces bright yellow at acidic pH and dim blue at neutral pH. Although the blue staining was relatively uninformative, we were able to monitor acidified compartments in each cell by visualizing the yellow fluorescence. Mock-infected cells had numerous acidic compartments, as evidenced by the multitude of bright yellow punctae (Fig. 6*A*). As expected, treatment with chloroquine caused all of the punctae to disappear (Fig. 6*B*). Interestingly, when cells expressing M2 were incubated with LysoSensor, a much smaller number of yellow compartments were present (Fig. 6*C*). Based on the trafficking assays described above, we hypothesize that these remaining punctae represent late endosomal and lysosomal compartments, as the function of these compartments is not compromised by M2 activity. We observed a similar staining pattern for all of the cells on the coverslip, suggesting that essentially all of the cells expressed M2. Within 15 min of addition of AMT to the M2-expressing cells, there was a dramatic increase in the number of acidic compartments, as evidenced by the appearance of numerous new yellow

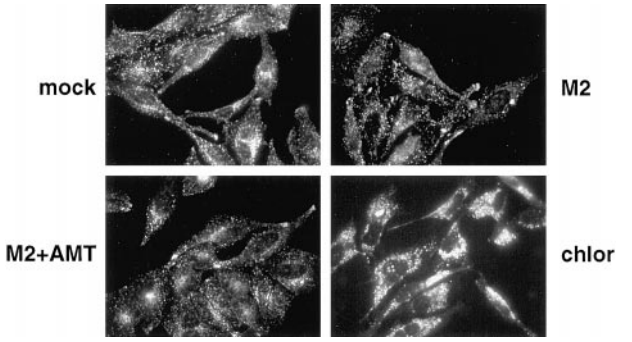

FIG. 5. **M2 does not affect the steady state distribution of lysosomal membrane proteins.** HeLa cells were mock-infected (*mock*) or infected with AV-TA and AV-M2 at a m.o.i. of 500 (*M2*). After infection, one dish of mock-infected cells was treated with 50 μg/ml chloroquine (*chlor*), and an AV-M2-infected dish was incubated with AMT (*M2+AMT*). The following day, cells were fixed and processed for indirect immunofluorescence to localize LAMP-1.

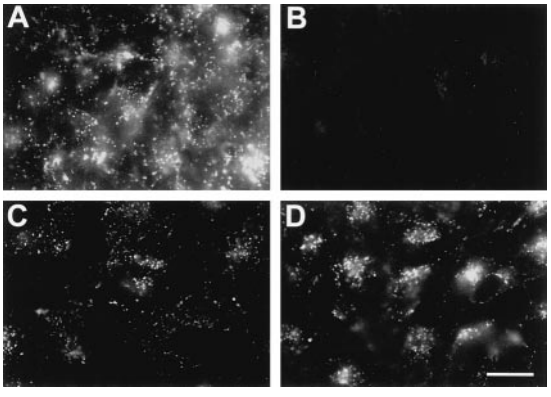

FIG. 6. **M2 expression perturbs the pH of a subset of acidified organelles.** HeLa cell grown on coverslips were incubated with LysoSensor, a pH-sensitive dye that fluoresces yellow in acidic compartments. Yellow fluorescence was compared in mock infected cells (*A*), cells treated with the weak base chloroquine (*B*), cells infected with M2 adenovirus at a m.o.i. of 500 (*C*), and M2-infected cells treated with the M2 ion channel blocker AMT (*D*). As expected, chloroquine treatment neutralizes all intracellular acidified compartments. By contrast, M2 expression causes a decrease in the number of acidic compartments, consistent with neutralization of the TGN and endosomes but not lysosomes. Acidification of juxtanuclear compartments is restored upon addition of AMT for 15 min. *Scale bar*: 10 μm.

punctae (Fig. 6*D*). Thus M2 expression alters the pH of a subset of acidified compartments in the cell, and the effects of M2 can be rapidly reversed.

M2 Expression Inhibits Lysosomal Delivery of Newly Synthesized Cathepsin D—Because we were able to selectively alter TGN or TGN/endosome function by varying M2 expression levels, we tested the effect of M2 on delivery of the newly synthesized lysosomal hydrolase cathepsin D. This protein is synthesized as a 53-kDa precursor (P) in the endoplasmic reticulum, clipped in the TGN and/or endosomes to an slightly smaller intermediate (I) form, then processed to a mature 30-kDa form (M) in lysosomes (31). Conversion to the mature form is not dependent on prior cleavage to the intermediate form (32). Pertubation of acidified compartments using various inhibitors blocks cathepsin D processing to the mature form and in some cases increases secretion of the precursor (33–38). However, because cathepsin D processing to its mature form requires acidic pH, it can be difficult to distinguish missorting of intracellular cathepsin D from the accumulation of precursor or intermediate forms in lysosomes. Therefore, we compared the effects of M2 and $BafA_1$ on processing and delivery of newly synthesized cathepsin D in HeLa cells (Fig. 7). As predicted, $BafA_1$ blocked proteolytic maturation of cathepsin D and

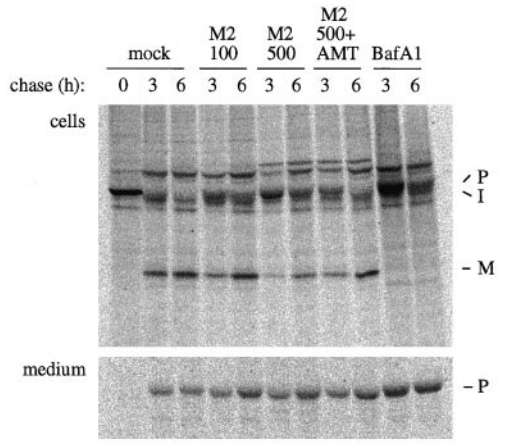

FIG. 7. **Effect of M2 on cathepsin D processing.** HeLa cells were infected with AV-M2 and AV-TA at the indicated m.o.i. The following day, cells were radiolabeled for 15 min, then chased for the indicated times. AMT (5 μM) and $BafA_1$ (1 μM) were added to the indicated dishes 30 min prior to radiolabeling. Cathepsin D was immunoprecipitated from the cells and medium as described under "Experimental Procedures." The migration of the precursor (*P*), intermediate (*I*), and mature (*M*) forms of cathepsin D is noted. On occasion, a slowly migrating band of unknown origin was observed in some samples.

slightly increased secretion of the precursor. Low expression levels of M2 (m.o.i. 100) slightly delayed processing of cathepsin D to both the intermediate and mature forms. Higher expression of M2 (m.o.i. 500) had a more dramatic effect on both steps that was almost completely reversed when AMT was included. These data suggest that at least some cleavage of cathepsin D to its intermediate form normally occurs in the TGN. Furthermore, because higher expression levels of M2 had a greater effect on cathepsin D maturation, a portion of cathepsin D may traffic through early endosomes in HeLa cells.

DISCUSSION

We have developed a new method to selectively elevate the pH of some intracellular acidified compartments. By varying the expression level of virally expressed influenza M2 protein, an acid-activated ion channel, we can reversibly modulate TGN or TGN/endosome pH in HeLa cells without affecting lysosomal pH or function. At low expression levels, maximal effects on TGN-to-cell surface delivery of the marker protein influenza HA were observed. However, higher expression levels were required to maximally inhibit the recycling of transferrin. Even at these high expression levels, no effects on lysosomal function were observed. Fluorescence staining of live cells using a pH-sensitive dye confirmed the selective effect of M2 on a subset of acidified compartments. To our knowledge, this is the first *direct* demonstration that influenza M2 perturbs organelle pH in mammalian cells.

Although even low expression levels of M2 dramatically inhibited TGN-to-cell surface delivery of the marker protein influenza HA, M2 did not completely block exit from the TGN, as secretion of newly synthesized cathepsin D continued normally in M2-expressing cells. Moreover, we have found that cell surface delivery of another heterologous membrane protein, the polymeric immunoglobulin receptor, was completely unaffected by even high levels of M2 expression.[3] The selective effect of M2 on HA but not polymeric immunoglobulin receptor delivery was also observed in polarized Madin-Darby canine kidney cells.[4] Differences in the marker proteins as well as cell lines used

[3] G. A. Gibson and O. A. Weisz, unpublished observations.
[4] J. R. Henkel, G. A. Gibson, and O. A. Weisz, unpublished observations.

could thus account for some of the discrepancies between the various studies on the role of acidification on secretory traffic.

Interestingly, the maximal effect of M2 on Tf recycling never approached that of the V-ATPase inhibitor $BafA_1$. Because essentially all cells are infected under our conditions, this difference does not reflect activity of M2 in only a subset of cells. Although it is possible that $BafA_1$ has a greater effect on endosomal pH than M2, increasing M2 m.o.i. 5-fold had no further effect on Tf recycling. Rather, our results suggest that M2 is present or active in only a subset of endocytic compartments through which receptor-bound Tf passes. Iron is thought to dissociate from Tf primarily in sorting endosomes; subsequently, receptor-bound Tf is segregated into recycling endosomes and returned to the cell surface. In the presence of $BafA_1$, iron remains bound to transferrin throughout the pathway and prevents recycled Tf from dissociating from its receptor upon return to the cell surface (15). In cells expressing M2, the pH of a subset of acidified compartments along the transferrin recycling route could be altered, resulting in partial dissociation of iron from transferrin during recycling. Alternatively, iron dissociation could proceed normally in M2-expressing cells and the effects we observed might reflect effects on the rate of receptor movement along the recycling pathway. Presley *et al.* (39) found that $BafA_1$ treatment caused a ~45% decrease in the rate of transferrin receptor recycling; this is comparable with the ~35% effect on transferrin release we observed at high levels of M2 expression.

Importantly, even at high expression levels, M2 had no effect on the kinetics of degradation of internalized EGF, suggesting that both delivery to lysosomes and lysosomal function were unaffected. By contrast, $BafA_1$ treatment has been variously reported to block delivery from late endosomes to lysosomes (15) and lysosomal degradation but *not* delivery to lysosomes (7). In addition, lysosome morphology and the steady state distribution of lysosomal enzymes were unaffected in M2-expressing cells. This is in sharp contrast to all other pH perturbants, which have dramatic effects on lysosome pH and function. The ability to alter the pH of a subset of intracellular compartments using M2 should thus help us to dissect the role of acidification in individual steps along pathways that involve transport through multiple acidified compartments.

To test the utility of our system, we examined the effect of M2 on delivery of newly synthesized cathepsin D to lysosomes. Because many steps in the sorting of lysosomal hydrolases are pH-sensitive, the role of acidification in individual compartments remains relatively poorly understood despite considerable study. Cathepsin D delivery to lysosomes first involves binding to mannose 6-phosphate receptors (MPRs) in the TGN. This step is complicated by the differential pH binding profiles of the two MPRs: the cation-dependent MPR binds many substrates weakly at neutral pH, while the cation-independent MPR is pH-insensitive within a relatively broad range (40). While the two MPRs have overlapping substrate specificities, they cannot completely substitute for each other when one is nonfunctional (41, 42). The MPR-hydrolase complexes are transported to late endosomes where pH-dependent dissociation of the hydrolases occurs. While a direct route from the TGN to late endosomes has been proposed, in some cell types cathepsin D may transit through early endosomes *en route* to lysosomes (43, 44). In addition to this pathway, a significant fraction of cathepsin D delivery in some cells also occurs via MPR-independent mechanisms (45, 46). $BafA_1$ treatment likely inhibits the pH-dependent steps; however, since cathepsin D maturation in lysosomes is also inhibited, it is difficult to determine the effect of $BafA_1$ on individual steps in transport or on MPR-independent delivery. Furthermore, neutralized lysosomes might not be recognized as an appropriate target for fusion by compartments carrying newly synthesized cargo; for example, inactivation of lysosomes using HRP blocks the lysosomal delivery of internalized EGF-EGF receptor complexes (47). Processing of newly synthesized cathepsin D to its mature form (a lysosomal event) was progressively inhibited by increased expression of M2 and completely inhibited (as expected) by $BafA_1$. The progressive effect of increasing M2 expression on cathepsin D processing and delivery supports the idea that some cathepsin D traffics through early endosomes in these cells. In neither case was cathepsin D delivery to lysosomes completely inhibited. The properly targeted fraction could represent cathepsin D transport via the pH-independent pathway or cathepsin D binding to the cation-independent MPR, which may still occur at neutral pH. Importantly, our data also demonstrate that inefficient delivery of newly synthesized hydrolases in pH-perturbed cells is not simply due to the loss of recognition of the lysosome as an appropriate target.

In summary, influenza M2 expression provides a novel method to selectively alter the pH of a subset of acidified organelles. Further characterization of the effects of M2 on pH in individual compartments should help us dissect the role of acidification in numerous processing and transport steps along the biosynthetic and endocytic pathways. In addition, the possibility of altering M2 localization or proton channel activity via site-directed mutagenesis may add a new level of flexibility in manipulating organelle pH.

Acknowledgments—We thank Mark Krystal for his gift of BL-1743, Robert Lamb for the anti-M2 antibody, Greg Conner for anti-cathepsin antibody used in unpublished studies, Gerard Apodaca for critical review of this manuscript, and Doug Fambrough and Nancy Gough for helpful suggestions.

REFERENCES

1. Xu, H., and Shields, D. (1994) *J. Biol. Chem.* **269,** 22875–22881
2. Chanat, E., and Huttner, W. B. (1991) *J. Cell Biol.* **115,** 1505–1519
3. Mukherjee, S., Ghosh, R. N., and Maxfield, F. R. (1997) *Physiol. Rev.* **77,** 759–803
4. Chatterjee, D., Chakraborty, M., Leit, M., Neff, L., Jamsa-Kellokumpu, S., Fuchs, R., and Baron, R. (1992) *Proc. Natl. Acad. Sci. U. S. A.* **89,** 6257–6261
5. Matsuoka, K., Higuchi, T., Maeshima, M., and Nakamura, K. (1997) *Plant Cell* **9,** 533–546
6. Temesvari, L. A., Rodriguez-Paris, J. M., Bush, J. M., Zhang, L., and Cardelli, J. A. (1996) *J. Cell Sci.* **109,** 1479–1495
7. Yoshimori, T., Yamamoto, A., Moriyama, Y., Futai, M., and Tashiro, Y. (1991) *J. Biol. Chem.* **266,** 17707–17712
8. Muroi, M., Shiragami, N., Nagao, K., Yamasaki, M., and Takatsuki, A. (1993) *Cell Struct. Funct.* **18,** 139–149
9. Yilla, M., Tan, A., Ito, K., Miwa, K., and Ploegh, H. L. (1993) *J. Biol. Chem.* **268,** 19092–19100
10. Palokangas, H., Metsikko, K., and Vaananen, K. (1994) *J. Biol. Chem.* **269,** 17577–17585
11. Johnson, L. S., Dunn, K. W., Pytowski, B., and McGraw, T. E. (1993) *Mol. Biol. Cell* **4,** 1251–1266
12. Harada, M., Shakado, S., Sakisaka, S., Tamaki, S., Ohishi, M., Sasatomi, K., Koga, H., Sata, M., and Tanikawa, K. (1997) *Liver* **17,** 244–250
13. Harada, M., Sakisaka, S., Yoshitake, M., Kin, M., Ohishi, M., Shakado, S., Mimura, Y., Noguchi, K., Sata, M., and Tanikawa, K. (1996) *J. Hepatol.* **24,** 594–603
14. van Weert, A. W. M., Geuze, H. J., and Stoorvogel, W. (1997) *Eur. J. Cell Biol.* **74,** 417–423
15. van Weert, A. W. M., Dunn, K. W., Geuze, H. J., Maxfield, F. R., and Stoorvogel, W. (1995) *J. Cell Biol.* **130,** 821–834
16. Sugrue, R. J., and Hay, A. J. (1991) *Virology* **180,** 617–624
17. Holsinger, L. J., and Lamb, R. A. (1991) *Virology* **183,** 32–43
18. Pinto, L. H., Holsinger, L. J., and Lamb, R. A. (1992) *Cell* **69,** 517–528
19. Chizhmakov, I. V., Geraghty, F. M., Ogden, D. C., Hayhurst, A., Antoniou, M., and Hay, A. J. (1996) *J. Physiol. (Lond.)* **494,** 329–336
20. Sakaguchi, T., Tu, Q., Pinto, L. H., and Lamb, R. A. (1997) *Proc. Natl. Acad. Sci. U. S. A.* **94,** 5000–5005
21. Wang, C., Lamb, R. A., and Pinto, L. H. (1995) *Biophys. J.* **69,** 1363–1371
22. Tu, Q., Pinto, L. H., Luo, G., Shaughnessy, M. A., Mullaney, D., Kurtz, S., Krystal, M., and Lamb, R. A. (1996) *J. Virol.* **70,** 4246–4252
23. Henkel, J. R., and Weisz, O. A. (1998) *J. Biol. Chem.* **273,** 6518–6524
24. Henkel, J. R., Apodaca, G., Altschuler, Y., Hardy, S., and Weisz, O. A. (1998) *Mol. Biol. Cell* **8,** 2477–2490
25. Sakaguchi, T., Leser, G. P., and Lamb, R. A. (1996) *J. Cell Biol.* **133,** 733–747
26. Takeuchi, K., and Lamb, R. A. (1994) *J. Virol.* **68,** 911–919
27. Ohuchi, M., Cramer, A., Vey, M., Ohuchi, R., Garten, W., and Klenk, H.-D.

(1994) *J. Virol.* **68,** 920–926
28. Grambas, S., Bennett, M. S., and Hay, A. J. (1992) *Virology* **191,** 541–549
29. Grambas, S., and Hay, A. J. (1992) *Virology* **190,** 11–18
30. Ciampor, F., Bayley, P. M., Nermut, M. V., Hirst, E. M. A., Sugrue, R. J., and Hay, A. J. (1992) *Virology* **188,** 14–24
31. Gieselmann, V., Pohlmann, R., Hasilik, A., and von Figura, K. (1983) *J. Cell Biol.* **97,** 1–5
32. Richo, G. R., and Conner, G. E. (1994) *J. Biol. Chem.* **269,** 14806–14812
33. Oda, K., Nishimura, Y., Ikehara, Y., and Kato, K. (1991) *Biochem. Biophys. Res. Commun.* **178,** 369–377
34. Imort, M., Zuhlsdorf, M., Feige, U., Hasilik, A., and von Figura, K. (1983) *Biochem. J.* **214,** 671–678
35. Rosenfeld, M. G., Kreibich, G., Popov, D., Kato, K., and Sabatini, D. D. (1982) *J. Cell Biol.* **93,** 135–143
36. Gonzalez-Noriega, A., Grubb, J. H., Talkad, V., and Sly, W. S. (1980) *J. Cell Biol.* **85,** 839–852
37. Nishimura, Y., Amano, J., Sato, H., Tsuji, H., and Kato, K. (1988) *Arch. Biochem. Biophys.* **262,** 159–170
38. Hasilik, A., and Neufeld, E. F. (1980) *J. Biol. Chem.* **255,** 4937–4945
39. Presley, J. F., Mayor, S., McGraw, T. E., Dunn, K. W., and Maxfield, F. R. (1997) *J. Biol. Chem.* **272,** 13929–13936
40. Hoflack, B., Fujimoto, K., and Kornfeld, S. (1987) *J. Biol. Chem.* **262,** 123–129
41. Pohlmann, R., Wendland, M., Boeker, C., and von Figura, K. (1995) *J. Biol. Chem.* **270,** 27311–27318
42. Kasper, D., Dittmer, F., von Figura, K., and Pohlmann, R. (1996) *J. Cell Biol.* **134,** 615–623
43. Ludwig, T., Griffiths, G., and Hoflack, B. (1991) *J. Cell Biol.* **115,** 1561–1572
44. Rijnboutt, S., Stoorvogel, W., Geuze, H. J., and Strous, G. J. (1992) *J. Biol. Chem.* **267,** 15665–15672
45. Diment, S., Leech, M. S., and Stahl, P. D. (1988) *J. Biol. Chem.* **263,** 6901–6907
46. von Figura, K., and Hasilik, A. (1986) *Annu. Rev. Biochem.* **55,** 167–193
47. Futter, C. E., Pearse, A., Hewlett, L. J., and Hopkins, C. R. (1996) *J. Cell Biol.* **132,** 1011–1023